JPn Neuroscience
The Journal of Physiology

Subpopulation-specific patterns of intrinsic connectivity in mouse superficial dorsal horn as revealed by laser scanning photostimulation

Masafumi Kosugi[1], Go Kato[1], Stanislav Lukashov[1], Gautam Pendse[2], Zita Puskar[3], Mark Kozsurek[3] and Andrew M. Strassman[1]

[1]*Dept. Anesthesia and Critical Care, Beth Israel Deaconess Med. Ctr. and Harvard Medical School, Boston, MA 02215, USA*
[2]*P.A.I.N. Group, McClean Hospital, Belmont, MA 02478, USA*
[3]*Department of Anatomy, Histology and Embryology Faculty of Medicine, Semmelweis University, H-1094 Budapest, Hungary*

Key points

- Sensory neurons that detect painful and non-painful stimulation of body tissues have axons that project to the dorsal horn of the spinal cord, where their terminations are partially segregated into superficial (I–II) and deep (III–IV) dorsal horn laminae, respectively.
- The dorsal horn contains many excitatory and inhibitory interneurons whose axons synapse on other dorsal horn neurons to enhance or suppress sensory transmission.
- This study used a localized stimulation technique (laser scanning photostimulation) for high-resolution mapping of synaptic connections between dorsal horn interneurons, in an *in vitro* 'slice' preparation of the mouse lumbar spinal cord.
- Some neurons in superficial layers of the dorsal horn have long dendrites that extend ventrally into deeper layers of the dorsal horn, and these neurons can receive excitatory or inhibitory synaptic input from neurons in the deeper layers.
- These interlaminar connections may be involved in interactions between transmission of signals underlying painful *versus* non-painful sensations.

Abstract The primary goal of this study was to map the transverse distribution of local excitatory and inhibitory synaptic inputs to mouse lamina I spinal dorsal horn neurons, using laser scanning photostimulation. A sample of lamina II neurons was also studied for comparison. Lamina I neurons received excitatory synaptic input from both laminae I–II and the outer part of III–IV, especially the II/III border region, while the inhibitory input zones were mostly confined within I–II. The excitatory synaptic input zones showed a pronounced medial asymmetry, which was correlated with a matching asymmetry in the dendritic fields of the neurons. Inhibitory input from laminae III–IV was found in a subpopulation of neurons occupying a highly restricted zone, essentially one cell layer thick, immediately below the lamina I/II border, with morphological and physiological properties that were distinct from other laminar populations in the superficial dorsal horn, and that suggest a critical role in interlaminar communication. This subpopulation also received excitatory input from laminae III–IV. Within this subpopulation, inhibitory III–IV input was correlated with the presence of long ventral dendrites. Correlations between the distribution of synaptic input zones and dendritic fields support the concept that interlaminar communication is mediated in part via contacts made onto ventrally extending dendrites of superficial laminae neurons. The results point to the presence of cell type specificity in dorsal horn circuitry, and

DOI: 10.1113/jphysiol.2012.244210

show how the study of connectivity can itself help identify previously unrecognized neuronal populations.

(Received 2 September 2012; accepted after revision 4 January 2013; first published online 7 January 2013)
Corresponding author A. Strassman: Dept. Anesthesia, CLS 647, Beth Israel Deaconess Med. Ctr., 3 Blackfan Circle, Boston, MA 02215, USA. Email: andrew_strassman@bidmc.harvard.edu

Abbreviations IR-DIC, infra-red differential interference contrast; LSPS, laser scanning photostimulation; NK1, neurokinin 1; sEPSC, spontaneous EPSC; SP, substance P.

Introduction

The superficial spinal dorsal horn (laminae I–II) is a major termination site for small diameter A-delta and C nociceptive primary afferent fibres (Light & Perl, 1979; Sugiura *et al.* 1986), and plays an essential role in the transmission and modulation of nociceptive sensory input to the CNS (Willis & Coggeshall, 2004; Todd, 2010). Lamina I contains a major population of ascending nociceptive projection neurons that are critically involved in the transmission of sensory inputs underlying pain behaviour and hypersensitivity (Craig & Kniffki, 1985; Mantyh *et al.* 1997; Nichols *et al.* 1999). The organization of primary afferent input to dorsal horn neurons has been examined in great detail (Light & Perl, 1979; Woodbury & Koerber, 2003; Braz *et al.* 2005; Dahlhaus *et al.* 2005; Zylka *et al.* 2005; Boada & Woodbury, 2008), but much less is known about the patterns of interneuronal connectivity within the dorsal horn. One basic question concerns the organization and origin of interlaminar connections. Such connections subserve both the transmission of nociceptive primary afferent input from superficial to deep laminae, as well as the transmission of non-nociceptive input from deep to superficial laminae. A further question concerns the organization of this circuitry at the level of specific cell types. A growing body of evidence supports the existence of cell type specificity in these interneuronal connections (Lu & Perl, 2003, 2005; Zheng *et al.* 2010; Torsney & MacDermott, 2006; Yasaka *et al.* 2007; Schneider, 2008; Luz *et al.* 2010; Zheng & Schneider, 2011), although this search is constrained by the current incomplete state of knowledge in identifying and defining the full constellation of cell types that exist in the dorsal horn (Todd, 2010). At the same time, it is possible that identifying patterns of connectivity between dorsal horn neurons might itself help in the ongoing attempt to define dorsal horn cell types.

In previous studies, we have used laser scanning photostimulation (LSPS) to show cell-type-specific patterns of local connectivity for lamina II neurons of rat dorsal horn (Kato *et al.* 2007, 2009). This method uses light-induced uncaging of glutamate as a stimulus to map the locations of local interneurons that give rise to synaptic inputs to a single morphologically identified postsynaptic neuron (Callaway & Katz, 1993; Katz & Dalva, 1994). Our prior studies were done mostly in parasagittal slices because the major lamina II cell types can only be distinguished in the parasagittal plane and, furthermore, connectivity in the transverse plane was found to be relatively sparse. The original goal of the present study was to focus specifically on mapping the inputs of lamina I neurons, for which transverse mapping was required, as these neurons can have mediolaterally oriented dendritic fields (Lima & Coimbra, 1986; Light *et al.* 1993; Galhardo & Lima, 1999). It was decided to switch to the mouse for the present study, partly because it was thought that the smaller size of this species might mean that more connectivity might be detected, as a larger proportion of the intrinsic circuitry would be contained in the limited depth of tissue ($\sim$100 μm in the z-axis) that is excited by the ultraviolet beam used for LSPS. The results did in fact show a robust connectivity in the transverse plane, with distinct patterns that could be correlated with differences in dendritic morphology and thus suggest the presence of subpopulations and cell-type-specific connectivity. The results also revealed a previously undemarcated zone immediately ventral to the lamina I/II border that contained neurons with properties that were distinct from those of other superficial dorsal horn neurons and that suggest a unique role in interlaminar circuitry.

Methods

All experimental procedures involving the use of animals were approved by the Institutional Animal Care and Use Committee of the Beth Israel Deaconess Medical Center. Methods for spinal cord slice preparation, whole-cell recording and LSPS were as described for the rat in Kato *et al.* (2009). The methods section of that paper discusses various methodological issues, including evidence that the glutamate uncaging stimulus does not activate axons of passage, and that the synaptically evoked responses are mostly monosynaptic.

Briefly, 21–24-day-old C57BL6 mice (Charles River Laboratories, Wilmington, MA, USA) were anaesthetized with urethane and decapitated, and a portion of the spinal cord was removed. Parasagittal slices of 250 μm or transverse slices of 400 μm thickness were prepared from the enlargement of the lumbar spinal cord with a vibratome (Vibratome 3000 Plus, Leica Biosystems, Buffalo Grove, IL, USA). The Krebs solution in the recording chamber

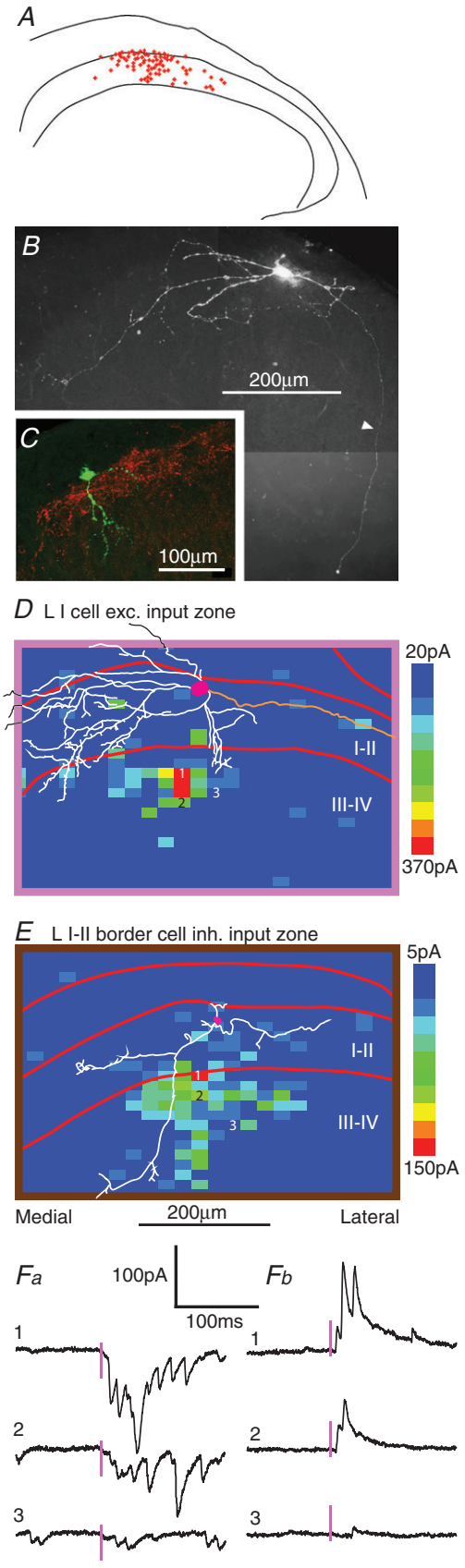

Figure 1.

A, locations of all the neurons for which mapping of synaptic input zones was done in transverse slices ($n = 77$), plotted on a drawing of the right dorsal horn. The borders of laminae I–II are shown. *B* and *C*, examples of intracellular staining of lamina I neurons. In *B*, the axon was visible (arrowhead). The neuron in *C* was located at the border between the NK1 band (red) and the overlying white matter. *D*, excitatory synaptic input zone of a lamina I neuron. Dendrites are white, soma is pink. The axon was also visible in this cell, and is shown in orange. *E*, inhibitory synaptic input zone of a lamina I–II border cell. The calibration bar also applies to *D*. Lateral is to the right in all images. *Fa,b*, examples of photostimulation-induced excitatory and inhibitory responses from the maps shown in *D* and *E*, respectively; the three traces (1–3) correspond to the marked stimulus sites in each map. The 3 ms stimulus is indicated by the pink bar.

contained (in mM): NaCl, 117; KCl, 3.6; $CaCl_2$, 2.5; $MgCl_2$, 1.2; NaH_2PO_4, 1.2; $NaHCO_3$, 25; glucose, 11. It also contained 100 μM 4-methoxy-7-nitroindolinyl caged L-glutamate (Tocris, St Ellisville, MO, USA). The patch pipettes (6–8 MΩ) were filled with a solution containing (in mM): potassium-gluconate, 136; KCl, 5; $CaCl_2$, 0.5; $MgCl_2$, 2; EGTA, 5; Hepes, 5; Mg-ATP, 5; for recording EPSCs in the voltage-clamp mode; Cs_2SO_4, 110; tetraethylammonium-chloride, 5; $CaCl_2$, 0.5; $MgCl_2$, 2; EGTA, 5; Hepes, 5; Mg-ATP, 5; for recording inhibitory outward currents in the voltage-clamp mode. Recordings were made using an Axon MultiClamp 700B amplifier (Molecular Devices, Union City, CA, USA). Laminar regions were visualized by infra-red differential interference contrast (IR-DIC) under 10× and 40× objectives. Blind whole-cell recordings were obtained from neurons at a depth of 50–100 μm in the slice. In some experiments, following the synaptic mapping with LSPS (described below), neurons were tested for a response of a slow inward current to bath application of substance P (SP; 2 μM for 1 min; Tocris, Bristol, UK). A fluorescent dye (Alexa Fluor 555 hydrazide, tris salt, 40 μM; Invitrogen, Eugene, OR, USA) was added to the pipette solution in order to visualize the neuron during the recording periods. Neurobiotin (0.1%; Vector, Burlingame, CA, USA) was also added for further anatomical examination following histological processing. Slices were fixed in 4% paraformaldehyde for 1–3 days. Neurobiotin was visualized by reacting with streptavidin conjugated to Alexa Fluor 555 or Alexa Fluor 488 (Invitrogen), and dendritic drawings were made from photomicrographs of stained cells (Fig. 1*B*).

The photostimulation apparatus (Prairie Technologies, Middleton, WI, USA) employed a continuous argon ion (UV) laser, as described in Kato *et al.* (2009). The laser beam was coupled to a fibre optic and transmitted through the 40× water immersion objective (NA 0.80) of an Olympus BX51WI microscope, to deliver 5 mW at the specimen. The microscope was mounted on an *x–y* motorized stage (Scientifica, Uckfield, East Sussex, UK),

while the tissue was mounted independently on a fixed platform. The stimulus site was changed by moving the entire microscope, so the laser beam was always centred within the microscope objective and the microscope field, and the optical properties of the stimulus were identical for all stimulus sites.

A critical methodological step that was carried out at the outset of our first LSPS studies in the rat was to test the effectiveness of the photostimulus for evoking action potentials in dorsal horn neurons, and determine the spatial resolution of the photostimulation (Kato *et al.* 2007). Because the evoking of synaptic responses by photostimulation requires the firing of action potentials in presynaptic neurons, the spatial resolution of the synaptic mapping is determined by the size of the surrounding area from which a neuron can be activated to threshold. This was determined by recording from a sample of dorsal horn neurons in current-clamp mode while mapping the locations of stimulus sites that were effective for evoking action potentials. Those studies showed that sites that were effective for evoking action potentials were primarily restricted to sites overlying or adjacent to the soma and most proximal dendrites. Thus, although the glutamate uncaging will also activate glutamate receptors on distal dendrites, that activation is relatively ineffective at exciting the neuron to threshold and so is expected to make only a minimal contribution to the synaptically evoked responses. For the present study, this action potential mapping was repeated for a sample of dorsal horn neurons in the mouse (Supplemental Fig. 1). Whereas the action potential mapping in the rat had been done while recording in whole-cell mode, the action potential recordings in the mouse were done in cell-attached mode, in order to avoid possible effects of the whole-cell recording configuration on neuronal excitability. Synaptic mapping was always done in whole-cell mode, under voltage-clamp conditions.

For synaptic mapping, the duration of the UV laser pulse was 3 ms and the caged glutamate concentration was 100 μM. A single photostimulus was delivered once to each site in a rectangular stimulation grid. Sites were stimulated in an order determined by a non-nearest neighbour algorithm to avoid desensitization, at 0.5–0.67 Hz. Spacing between sites in the stimulation grid was 15 μm dorsoventrally, 25 μm mediolaterally (in transverse slices) and 50 μm rostrocaudally (in parasagittal slices). Excitatory and inhibitory synaptic responses to photostimulation were recorded in separate experiments, under voltage-clamp conditions. Excitatory (inward) and inhibitory (outward) currents were recorded at holding potentials of −70 and 0 mV, respectively. Synaptic events as well as direct responses were detected with the aid of MiniAnalysis software (Synaptosoft, Fort Lee, NJ, USA) and confirmed by visual inspection. Peak amplitude and time of onset were determined for each event. Responses evoked by direct (non-synaptic) glutamate-induced currents in the recorded neurons and those evoked synaptically as a result of suprathreshold excitation of presynaptic neurons were distinguished by a latency criterion, as determined previously by Kato *et al.* (2007). In that study, it was found that direct responses to glutamate uncaging occur only at onset latencies shorter than 6 ms. Therefore, the synaptic response amplitude for each trial (each stimulation site) was measured as the sum of the peak amplitudes of all of the synaptic events whose onset occurred within the time window of 6–106 ms, relative to stimulus onset. Spontaneous activity was measured during the 100 ms pre-stimulus interval of each stimulus trial. A moving average of spontaneous activity was then calculated from the pre-stimulus activity over 100 stimulus trials. This moving average of spontaneous activity was then subtracted from the activity measured in the response time window to obtain the net response in each trial.

A colour-coded contour map was made for each neuron showing the amplitude of the synaptic response evoked from each stimulation site in the photostimulation scanning grid (Fig. 1*D*–*F*). When combining individual maps to make population averages, the response amplitudes of individual neurons were normalized based on peak response amplitude in order to equalize their contribution to the averaged map. For construction of averaged maps, individual maps were aligned dorsoventrally either by soma location or by laminar borders. For averaging of parasagittal maps, as in our prior studies (Kato *et al*. 2009), a straightening procedure was done on the individual maps prior to combining them for averaging, in order to make the laminar borders straight and perfectly horizontal. This procedure involves measuring the dorsoventral position of the lamina II/III border at each rostrocaudal position, and then shifting the dorsoventral coordinates of each column of stimulus sites dorsally or ventrally so that the dorsoventral coordinate of the lamina II/III border has the same value at all rostrocaudal positions. As part of this straightening procedure, the dorsoventral dimension of each individual map is adjusted so that the dorsoventral width of laminae I–II is standardized to a uniform value at all rostrocaudal positions for all of the individual maps. In our previous study, in which the sample of transverse maps was very small, no straightening procedure was devised for the transverse maps, and consequently no transverse averaged maps were constructed with alignment by laminar borders. For the present study, a straightening procedure was used for the transverse maps that was similar to that used for the parasagittal maps, but it included one extra step prior to the straightening. Because the superficial laminae are curved in the transverse plane, each map was rotated clockwise or counterclockwise if necessary to make the superficial laminae horizontal at

the neuron's position. Consequently, the vertical axis in the averaged maps does not strictly correspond to the dorsoventral axis of the dorsal horn, but instead corresponds to the 'outer-to-inner' axis of the dorsal horn laminae, whose slant relative to the dorsal–ventral axis varies somewhat across different mediolateral positions. The same rotation angle that was used for the synaptic input map for each neuron was also used to rotate the dendritic drawing for that neuron, prior to quantitative analysis. Thus, throughout this study, in the text as well as the averaged maps, the term 'dorsoventral' when applied to the transverse data actually denotes the outer-to-inner axis rather than the true dorsoventral axis. The amount of rotation needed for most neurons was relatively small ($<$15 deg), because the electrode sampling was done at an intermediate position along the mediolateral axis (Fig. 1*A*) where the laminae are most nearly horizontal.

For each neuron, a plot was made of the amplitude of the evoked responses along each axis (e.g. for a mediolateral plot, each point represents the sum of the response amplitudes across all dorsoventral positions, for a given mediolateral position). From these plots, a weighted mean was then calculated for each neuron, along each axis, as a way to represent the position of the synaptic input zone (Kato *et al.* 2009). In addition, a weighted mean was also calculated for each dendritic drawing, for each axis. This was done by converting the dendrite drawing into a black-and-white pixel (TIF) image, and calculating the weighted mean of the distribution of black pixels. The map rotation and the dendritic weighted mean calculation were done with custom software in Matlab (The MathWorks, Natick, MA, USA). The map straightening was done with custom software in LabView (National Instruments, Austin, TX, USA). Statistical comparisons were done by unpaired *t* test, one-way ANOVA and Chi-square test. Measurements are reported as mean $\pm$ SD.

Initially, an attempt was made to assign laminar location for each stained neuron to either lamina I or lamina II by examination of IR-DIC images of the live slice, as well as brightfield and darkfield images of the fixed slice as viewed both in water and in mounting media. Staining for the neurokinin 1 (NK1)-immunoreactive band in lamina I was also done in some slices (Fig. 1*C*), using rabbit anti-NK1 primary antibody (Sigma, St Louis, MO, USA), 1:10,000, with donkey anti-rabbit conjugated to Alexa Fluor 555 (Invitrogen). (NK1 immunoreactivity was not detected in any of the recorded neurons, possibly due to inadequate tissue fixation and preservation.) However, the laminar position was ambiguous for a substantial portion of the sample, in that some portion of the soma appeared to at least partially overlap the lamina I/II border. It was finally decided to simply make a measurement for each neuron of the distance from the dorsal edge of the soma to the white matter border, from IR-DIC and fluorescent images taken of the live slice during recording. These measurements were made blinded to the results of the synaptic mapping. These measurements were then used as the criteria for subdividing the sample into laminar groupings.

Results

LSPS was used to map excitatory and inhibitory synaptic input zones (in separate neurons) of superficial dorsal horn neurons in both transverse and parasagittal slices, in young mice (21–24 days old). Neurons that were just ventral to lamina I, within one cell diameter of the lamina I–II border (with the dorsal edge of their soma touching or nearly touching the I–II border), were grouped separately from the other lamina II neurons, and are here termed 'lamina I–II border' cells. We have not termed this region IIo because the latter term encompasses a larger portion of lamina II.

Unlike our prior data in the rat, where input zones in the transverse plane were spatially restricted and relatively sparse, the transverse maps in the mouse revealed robust connectivity, with heterogeneity and distinct patterns that point to the presence of subpopulations. Lamina I neurons received excitatory input from both lamina I–II and the outer part of III–IV, with the peak input coming from the II/III border region (Fig. 1*C*), while the inhibitory zones were mostly confined within I–II (Fig. 2*A* and *D*). The population average of the excitatory synaptic input zones for the lamina I neurons showed a pronounced medial asymmetry (Fig. 2*A* and *H*). Such an asymmetry was not present in the inhibitory input zones of the lamina I neurons, or in the excitatory or inhibitory input zones of the lamina II or lamina I–II border neurons (Fig. 2*B–F* and *H*). A matching medial asymmetry was found in the dendritic fields of the lamina I neuron population (Figs 3*A*, 4*Ad* and 5*B*). This population asymmetry in the dendrites resulted from a subset of neurons with dendrites that extended further in the medial *versus* the lateral direction, either because of relatively short lateral dendrites (e.g. neurons in column 1 in Fig. 3*A*) or because of medial or ventral curvature of lateral dendrites (e.g. first two neurons in columns 3 and 4 of Fig. 3*A*). Within the lamina I neuron population, the dendritic asymmetry was correlated with the asymmetry in the excitatory input zones ($r = 0.59$, $P < 0.01$; Fig. 5*B*). However, some medial asymmetry of the excitatory synaptic input zone was present even in neurons whose dendritic field was symmetric (i.e. in Fig. 5*B*, note the negative *y*-values of the points whose *x*-values are near 0).

The lamina I–II border cell population differed in its synaptic input zones from the cells above and below it in lamina I and II. Inhibitory input from laminae III–IV was

found in a subset of neurons that were all contained in the I–II border region (Figs 1*E* and 2*E*). The neurons in this region were heterogeneous, and only the subgroup of neurons with relatively long ventral dendrites received the inhibitory laminae III–IV input. Neurons with long ventral dendrites were also present in the remainder of lamina II, but only those in the I–II border region received the inhibitory input from III–IV. There

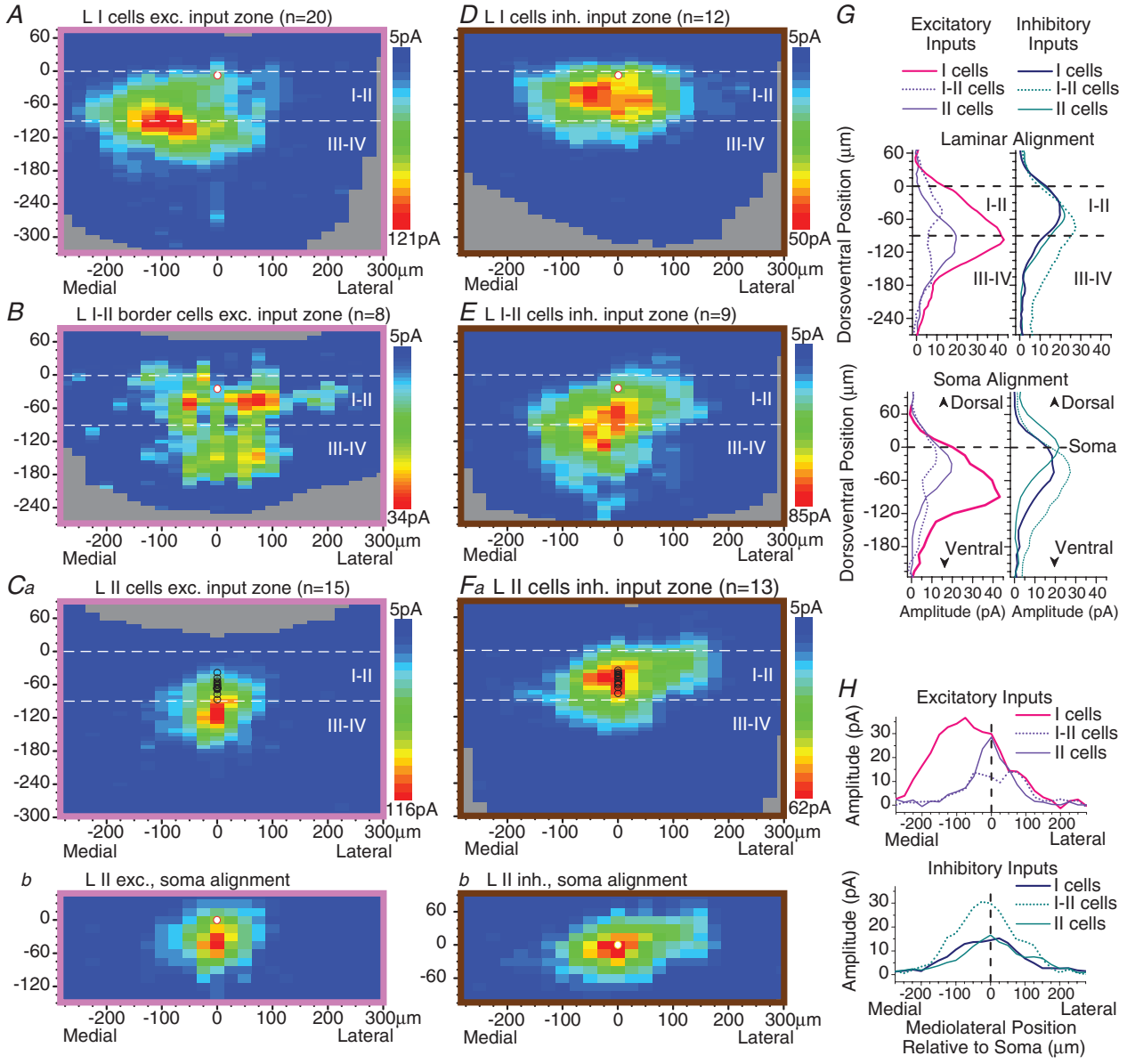

Figure 2.
A–F, averaged transverse maps of excitatory (*A–C*) and inhibitory (*D–F*) synaptic input zones for lamina I cells (*A* and *D*), 'lamina I–II border' cells (*B* and *E*) and lamina II cells (*C* and *F*). The 'I–II border' cells are located in a very restricted zone in the outermost part of lamina II, essentially one cell layer in width, with the dorsal edge of their soma touching or nearly touching the inner border of lamina I. For the lamina I cells and the laminae I–II border cells, the soma locations of each of these two populations are confined within a very narrow dorsoventral range, and so the soma locations of the recorded (postsynaptic) neurons in each map are marked by a single white circle (*A, B, D* and *E*). However, the sample of lamina II neurons is spread over a much larger dorsoventral range, and so the soma location of each neuron in the sample is marked individually with circles (*Ca* and *Fa*). In addition, a separate set of 'soma-aligned' averaged maps is shown for the lamina II neurons (*Cb* and *Fb*), in which the maps of the individual neurons were aligned dorsoventrally by soma location rather than by laminar borders (same colour scales as in *Ca* and *Fa*, respectively). *G* and *H*, plots of the dorsoventral (*G*) or mediolateral (*H*) distribution of synaptic response amplitudes for each of the averaged maps shown in *A–F*. In *G*, plots are shown with dorsoventral alignment by laminar borders (upper plots) and by soma position (lower plots).

was a significant correlation between the dorsoventral distribution of the dendritic field and the dorsoventral distribution of the inhibitory synaptic input zone for the lamina I–II border cells ($r = 0.68$, $P < 0.05$) as well as the lamina I cells ($r = 0.68$, $P < 0.05$), but not for the lamina II cells (Fig. 5*C*).

The I–II border population was also distinctive in that it contained neurons with more ventrally located excitatory

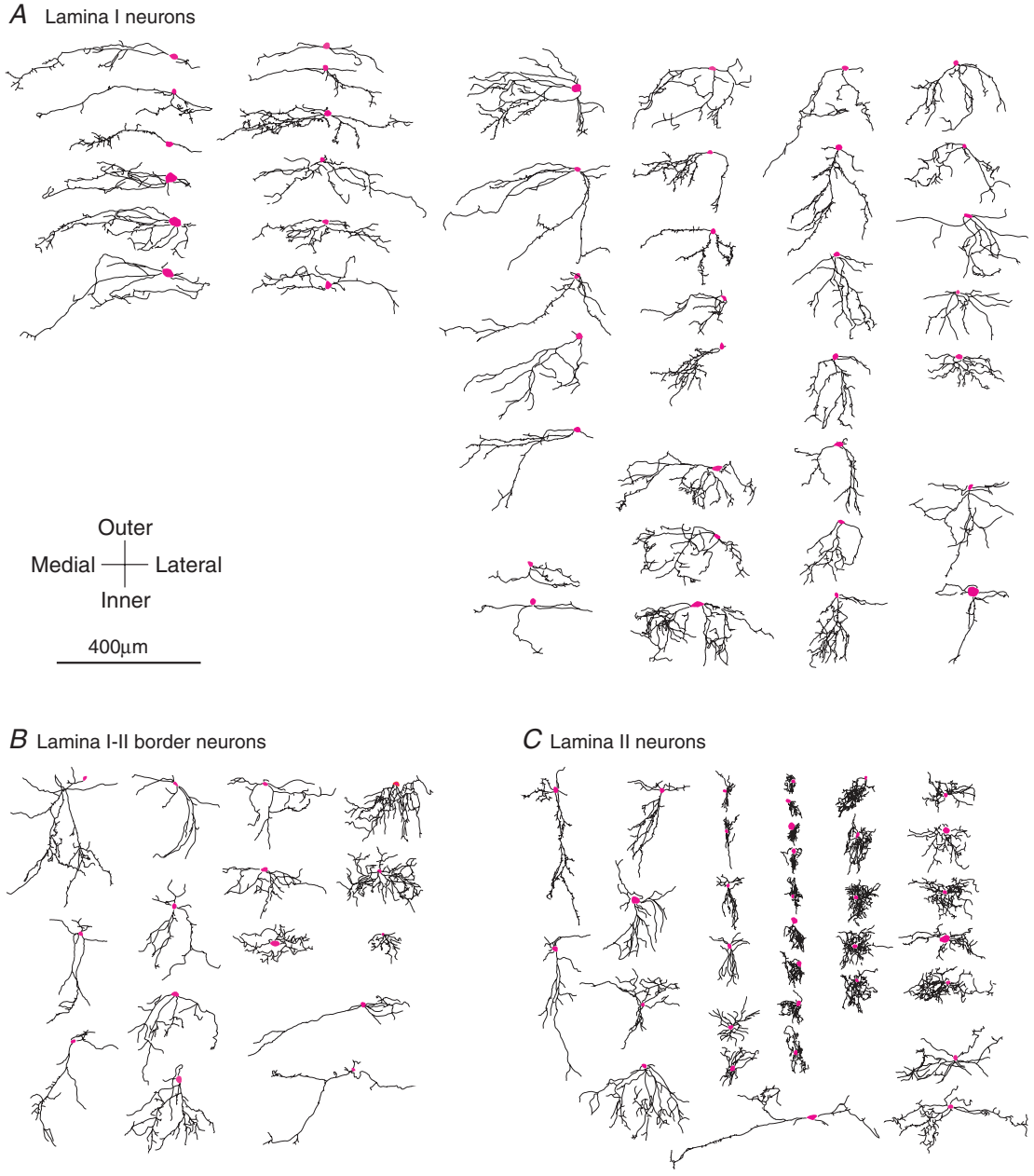

Figure 3.
Two-dimensional drawings of all of the stained neurons for which synaptic maps were obtained in transverse slices, divided into the three groups defined by laminar location (*A*, lamina I neurons; *B*, lamina I–II border neurons; *C*, lamina II neurons). A few neurons with poor dendritic staining were excluded. In addition, several neurons that were stained but for which synaptic mapping was not successful are included in this figure and in the anatomical analysis. Because dorsal horn laminae are not strictly horizontal in the transverse plane, each drawing was rotated clockwise or counterclockwise if necessary to make the dorsal horn laminae horizontal at the neuron's position. Consequently, the vertical axis in the figure does not strictly correspond to the dorsoventral axis of the dorsal horn, but instead corresponds to the 'outer-to-inner' axis of the dorsal horn laminae, whose slant relative to the dorsal–ventral axis varies somewhat across different mediolateral positions. Somas are pink. Although axons could be identified for some neurons, they are omitted from this figure.

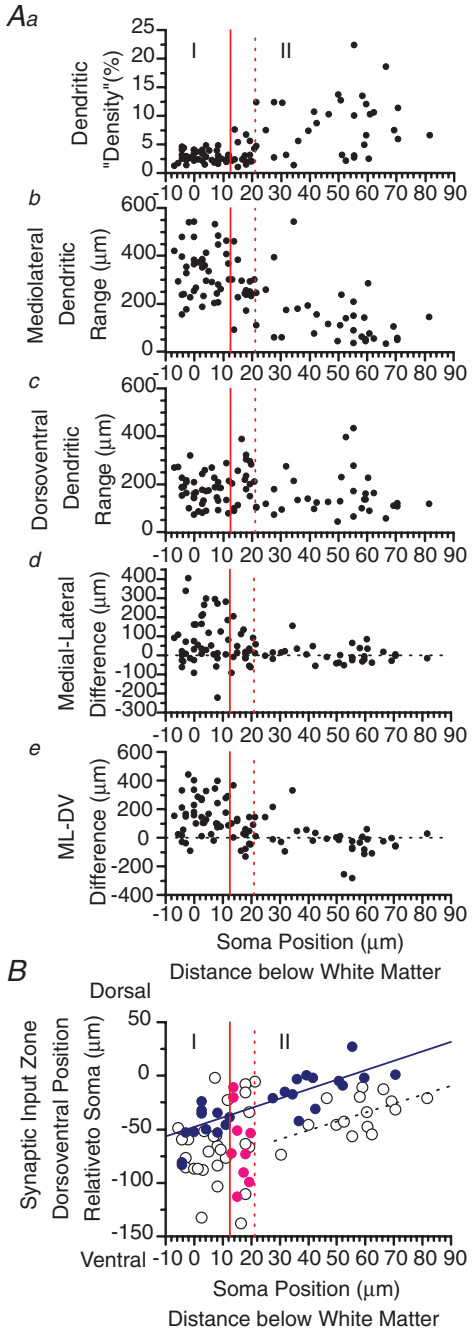

Figure 4.
Aa–e, scatterplots showing the variation in different dendritic parameters with laminar position of the neuron as measured by distance below the white matter, for the neurons shown in Fig. 3. The distance is measured from the dorsal edge of the soma. The solid red vertical line in each plot marks the approximate position of the inner border of lamina I, and the dotted red vertical line marks the inner border of the 'lamina I–II border' region. 'Density' (*a*) is an artificial measurement made by converting the dendritic drawing into a black-and-white pixel image and calculating the percentage of black pixels within a rectangle that encloses the dendritic field. The neurons with high 'density' are the ones with compact, bushy dendritic trees, as viewed in the transverse plane (i.e. fourth and fifth columns of lamina II neurons in Fig. 3.). *b* and *c*, total dendritic expanse ('range') in the mediolateral and dorsoventral axis, respectively. *d*, difference between the medial and lateral dendritic range. *e*, difference between the mediolateral and dorsoventral dendritic range; large positive values represent the neurons with mediolaterally oriented, dorsoventrally flattened dendritic fields. *B,* plot of the dorsoventral position of the synaptic input zone relative to the recorded neuron's soma *versus* soma position. Excitatory and inhibitory input zones are represented by open and filled circles, respectively. A regression line (solid blue line) is drawn for the inhibitory input zones of lamina I and lamina II neurons (blue circles), excluding the lamina I–II border neurons (pink circles) ($r = 0.81$, slope $= 0.88$, $P < 0.0001$; i.e. neurons that are more dorsal have inhibitory input zones displaced further ventrally from their soma). The lamina I–II border region contains neurons whose inhibitory input zones are further ventral relative to their soma than those of the other lamina II neurons. A second regression line (dotted black line) is drawn showing a similar relationship for the excitatory input zones of the lamina II neurons, excluding the I–II border neurons (open circles with soma position more than 22 μm below the white matter; $r = 0.57$, slope $= 0.83$, $P < 0.05$); this regression line is nearly parallel to but displaced ventrally from the line for the inhibitory input zones. The lamina I–II border population again differs from the remainder of the lamina II population in that its excitatory input zones do not fall along this line, because this population includes neurons with either more dorsal or more ventral excitatory input zones than are found in the remainder of lamina II.

input zones (relative to the soma) than other lamina II neurons (Fig. 4*B*), resulting in a substantial excitatory input from lamina III–IV (Fig. 2*B*). Unlike the inhibitory input zones, the dorsoventral position of the excitatory input zone was not correlated with the distribution of the dendritic field, in either the lamina I–II border cells or the lamina I cells; however, this correlation was significant for the remainder of the lamina II population (i.e. excluding the I–II border cells; $r = 0.60$, slope $= 0.32$, $P < 0.05$). Although the prior study in the rat did not make dendritic measurements, a similar correlation was found in that study for lamina II neurons, using the direct response to glutamate as an indirect indication of the dendritic distribution (fig. 5G of Kato *et al.* 2009).

Although the lamina I–II border cell population was morphologically heterogeneous (Fig. 3*B*), the population as a whole was distinguished morphologically from the other groups by the fact that it lacked the neurons with very dense, compact dendritic fields (as viewed in the transverse plane) that are present throughout the remainder of lamina II (Figs 3*C* and 4*Aa*), and also mostly lacked the mediolaterally oriented, dorsoventrally flattened dendritic fields that are common in lamina I (Figs 3*A*, 4*Ae* and 5*A*).

The other lamina II neurons (excluding the lamina I–II border cells) had inhibitory input zones that were relatively homogeneous. Their input zones tended to be at a similar dorsoventral position to the neuron's soma (Figs 2*Fb*, *G*, 4*B* and 5*C*), and so were mostly restricted to lamina II (Fig. 2*Fa* and *G*). The excitatory input zones

tended to be positioned slightly ventral to the neuron's soma (Figs 2*Cb*, *G* and 4*B*), and as a consequence the population average shows excitatory input from laminae III–IV as well as I–II (Fig. 2*Ca* and *G*). Because the sample of lamina II neurons is spread over a larger dorsoventral range than the samples of lamina I and lamina I–II border cells, separate averaged maps are shown for the lamina II neurons in which the maps of the individual neurons were aligned dorsoventrally by soma location rather than by laminar borders (Fig. 2*Cb* and *Fb*). Figure 4*B* illustrates an additional feature of the relationship between soma position and synaptic input zone position relative to the soma. A regression line (solid blue line) is drawn for the inhibitory input zones of lamina I and lamina II neurons (blue filled circles), excluding the lamina I–II border neurons (pink circles), showing that neurons that are more dorsal have inhibitory input zones that are displaced further ventral relative to their soma ($r = 0.81$, slope $= 0.88$, $P < 0.0001$). The lamina I–II border neurons do not fall along this regression line, in that their inhibitory input zones are displaced further ventrally relative to their soma. A similar relationship is shown by the second regression line (dotted black line) for the excitatory input zones of the lamina II neurons (excluding the I–II border neurons). This regression line is nearly parallel but displaced ventrally from the line for the inhibitory zones, reflecting the more ventral distribution of excitatory *versus* inhibitory zones noted above for lamina II neurons. An additional difference between the inhibitory and excitatory input zones of lamina II neurons is that the inhibitory zones had a greater mediolateral width (Fig. 2*C* and *F*; 419 ± 126 μm *vs.* 320 ± 128 μm, $P < 0.05$).

Peak amplitude

The peak amplitude of the excitatory synaptic input varied across the populations (note the differences in the maximum amplitude of the colour scales for the different plots in Fig. 2*A–Ca*). Relatively low response amplitudes were exhibited by the neurons throughout the I–II border region and also the outer part of lamina II (extending down to about 55 μm below the white matter), while the populations in lamina I and the more inner part of lamina II (about 55–85 μm below the white matter) exhibited greater variation, but included substantial numbers of neurons with higher amplitudes. Statistical comparison of these four groupings showed that both the population of I–II border cells as well as the neurons in the outer part of lamina II were significantly lower in their response amplitudes than the lamina I cells ($P < 0.01$ for both comparisons) or the cells in the inner part of II ($P < 0.05$ for both comparisons). The peak amplitudes for the four groups were 261 ± 163, 103 ± 79, 74 ± 47 and 240 ± 112 pA, for I, I–II, outer II and inner II, respectively. (Note that this further demarcation of outer and inner II was done by *post hoc* observation of the response amplitudes, not by anatomical criteria, and was not done for the other analyses in this study. Separate averaged maps are not shown for these two further subgroupings within lamina II because there was no apparent difference in the spatial distribution of inputs, only their amplitudes.) The amplitudes of peak inhibitory responses did not show significant variation between groups. It was also noted that the frequency of spontaneous EPSCs (sEPSC) was correlated with peak excitatory response amplitude ($r = 0.55$, $P < 0.0001$), and

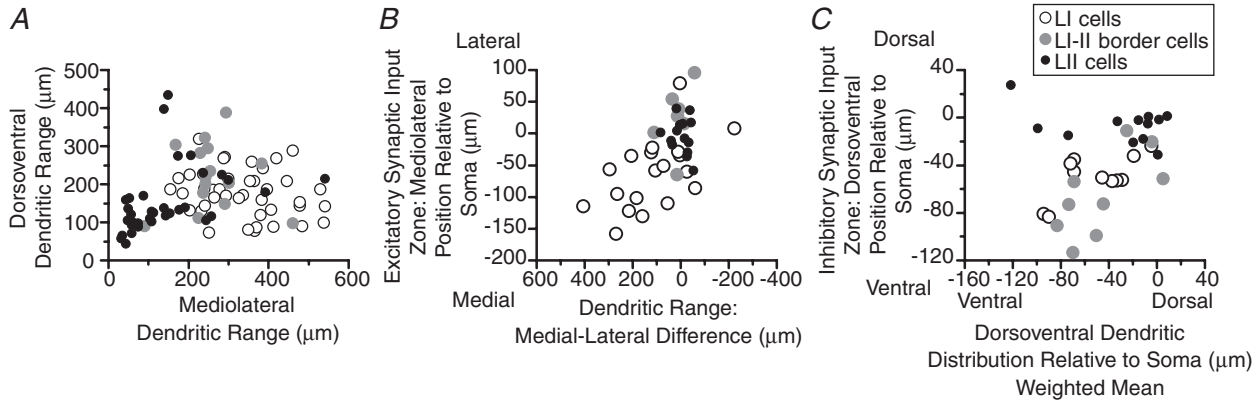

Figure 5.
Anatomical/physiological relations. *A*, dorsoventral *versus* mediolateral dendritic range. *B*, correlation of mediolateral asymmetry, as shown by plot of mediolateral position of excitatory input zone relative to soma (weighted mean) *versus* the difference between the medial and lateral dendritic range. The correlation is significant for the lamina I neurons ($r = 0.59$, $P < 0.01$). A weaker but significant correlation is also found if one uses the mediolateral weighted mean of the dendritic distribution instead of the mediolateral difference ($r = 0.45$, $P < 0.05$). *C*, dorsoventral position of the inhibitory synaptic input zone (weighted mean) relative to the soma *versus* dorsoventral weighted mean of the dendritic distribution. A significant correlation is shown by the lamina I neurons ($r = 0.68$, $P < 0.05$) and the lamina I–II border neurons ($r = 0.68$, $P < 0.05$), but not the lamina II neurons.

that sEPSC frequency showed a similar pattern of variation between these four laminar groupings as was found for the peak amplitude of the excitatory synaptic input: neurons with relatively low sEPSC frequency were present throughout laminae I–II, while neurons with relatively higher sEPSC frequency (>11 Hz) were present primarily in lamina I and inner II. The percentage of neurons with sEPSC frequency greater than 11 Hz was 48%, 0%, 8% and 42% for I, I–II, outer II and inner II, respectively ($P < 0.01$, Chi-square). The mean sEPSC frequency for these four groups was 12.1 ± 7.3, 5.8 ± 4.1, 3.9 ± 2.0 and 9.7 ± 6.9, respectively ($P < 0.05$, ANOVA). For the entire sample, mean sEPSC and spontaneous IPSC frequency was 9.4 ± 6.8 and 3.3 ± 2.7, respectively ($P < 0.0001$, *t* test).

Parasagittal synaptic input maps

In addition to the transverse maps described above, synaptic input maps of lamina I cells were also obtained in parasagittal slices (Fig. 6*A* and *D*). As with the neuronal sample obtained in transverse slices, a subset of neurons in the sample was judged to be just below the lamina I border, with the dorsal edge of their soma touching or nearly touching the I–II border, and are grouped separately as lamina I–II border cells (Fig. 6*B* and *E*). In addition, a small number of neurons in the parasagittal sample was at a slightly more ventral position, about one cell diameter below the inner border of lamina I, and are here grouped separately as IIo cells (Fig. 6*C* and *F*). This small sample of IIo neurons is not comparable to the much larger and dorsoventrally more extensive sample of lamina II neurons that was obtained in transverse slices.

As was observed in the transverse maps, the lamina I–II border cells received a substantial excitatory input from lamina III–IV (Fig. 6*B*). However, unlike the transverse data, the sample of lamina I–II border cells that was mapped for inhibitory inputs did not show a substantial inhibitory input from lamina III–IV (Fig. 6*E*). This sample

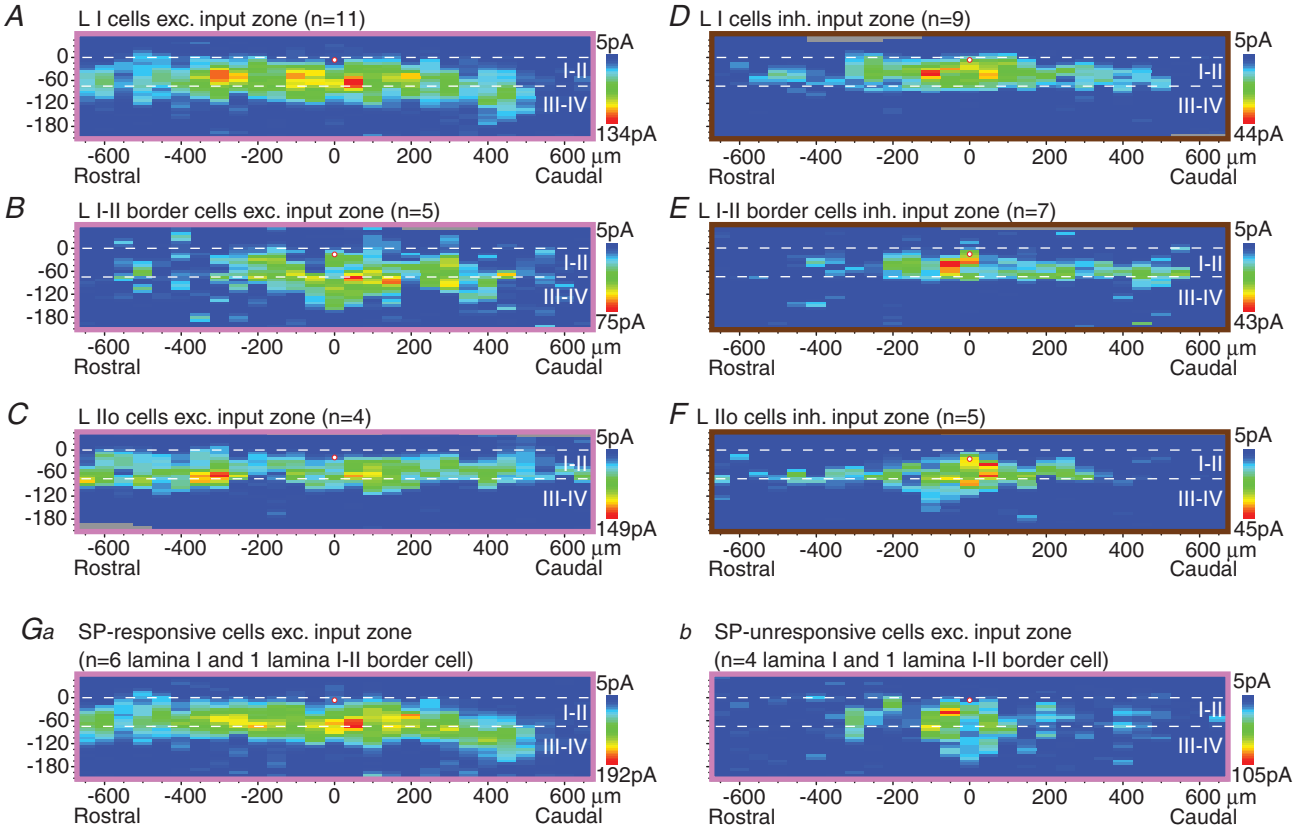

Figure 6.
A–F, averaged parasagittal maps of excitatory (*A–C*) and inhibitory (*D–F*) synaptic input zones for lamina I cells (*A* and *D*), lamina I–II border cells (*B* and *E*) and lamina IIo cells (*C* and *F*). As in the transverse sample (Fig. 2), the I–II border cells are about one cell diameter below the white matter. The small sample of IIo cells in this figure is restricted to the outermost part of lamina II, just slightly below the I–II border cells (about one cell diameter below the I–II border), and so is not comparable to the larger and dorsoventrally more extensive sample of lamina II cells collected in transverse slices (Fig. 2*C* and *F*). *Ga,b*, averaged excitatory synaptic input zones of cells responsive and unresponsive to substance P (SP), respectively; only lamina I and lamina I–II border cells are included. Note that the parasagittal maps have a smaller scale than the transverse maps (Fig. 2).

differed from the transverse sample of lamina I–II border cells in that it contained only one neuron with relatively long ventral dendrites, which was the morphological feature that was associated with lamina III–IV input in the transverse sample. However, the parasagittal inhibitory maps revealed one additional distinguishing feature of the lamina I–II border cells: the inhibitory input zones of the individual neurons had a significantly smaller rostrocaudal extent than those of the lamina I neurons (564 ± 393 μm *vs.* 950 ± 249 μm, $P < 0.05$; this is a property of the individual maps and is not apparent from viewing the population averages in Fig. 6).

SP responsiveness

Of the 20 neurons whose excitatory input zones were mapped in parasagittal slices, 15 were tested for a direct response (slow inward current) to bath application of SP (2 μM for 1 min) following the synaptic mapping. A response to SP was found in 7/15 neurons tested (6/10 lamina I cells, 1/2 lamina I–II border cells, 0/3 lamina IIo cells; peak response amplitude 14–63 pA). The excitatory synaptic input zones of the SP-responsive and unresponsive neurons were compared, excluding the 3 SP-unresponsive IIo neurons (Fig. 6*Ga,b*). The SP-responsive neurons had input zones with a larger rostrocaudal extent (500 ± 325 *vs.* 150 ± 150 μm, $P < 0.05$, for rostrocaudal 'half-width', or extent of region encompassing sites whose amplitude is at least half of the maximum), and also had a larger peak amplitude in their excitatory synaptic responses (401 ± 177 *vs.* 175 ± 100 pA, $P < 0.05$). These two groups were not significantly different in mean sEPSC frequency (21.5 ± 15.4 *vs.* 7.8 ± 4.7 for SP-responsive *vs.* -unresponsive neurons, $P = 0.10$, *t* test). However, the proportion of neurons with high sEPSC frequency (>12 Hz) was greater in the SP-responsive group (5/7 *vs.* 0/5 neurons, $P < 0.05$, Chi-square). The SP-responsive and -unresponsive groups were both heterogeneous in their dendritic morphology.

Discussion

The present study used LSPS to map the location of local synaptic inputs to superficial dorsal horn neurons in the mouse. The neuronal sampling in our previous LSPS studies in the rat was primarily concentrated in lamina II, and was done almost entirely in the parasagittal plane, as it appeared that this was the predominant orientation of the intrinsic connectivity in the superficial laminae (Kato *et al.* 2007, 2009). The sample of lamina I neurons in these prior studies, all in the parasagittal plane, was too small to investigate the presence of subpopulations or morphophysiological correlations. The original purpose of the present study was to obtain a more complete sample of lamina I neurons, including transverse mapping, to allow a more quantitative population analysis, as well as an examination of mediolateral organization. The switch from rat to mouse was done partly in the hope that more connectivity would be revealed (see Introduction), particularly in the transverse plane, and this did appear to be the case. The unexpected results, including the mediolateral asymmetry found in lamina I neurons, prompted us to extend our transverse sampling to include lamina II as well, in order to clarify the nature of the laminar-specific population differences we observed in the transverse maps.

Based on our results, we propose that there is a highly restricted zone, essentially one cell layer thick, immediately below the lamina I–II border whose neuronal population, although heterogenous, has properties that are distinct from those of the cells in the remainder of lamina II, and even the remainder of IIo, as well as from lamina I. The most unique distinguishing feature of this region was inhibitory input from laminae III–IV. While some lamina I cells had inhibitory input zones that extended slightly across the laminae II/III border, distinct inhibitory input zones with their peak in laminae III–IV were found only for cells in this lamina I–II border region. Among cells in this region, but not in the remainder of lamina II, inhibitory input from laminae III–IV correlated with the presence of long ventral dendrites. Cells with long ventral dendrites were also present deeper in lamina II, but those cells received inhibitory input only from positions that were dorsoventrally close to their soma, a pattern that is relatively invariant for all morphological cell types throughout lamina II, other than the I–II border region. Cells in this border region also received excitatory input from laminae III–IV and, although they are not unique in that respect, the population differed from that in the remainder of lamina II in containing cells whose excitatory input zones were displaced further ventrally relative to the neuron's soma. The population also differed from that in the remainder of lamina II in that, like lamina I, it lacked the subpopulation of neurons with extremely dense, compact dendritic fields, as viewed in the transverse plane. While the lamina I–II border population had some morphological features in common with the population in lamina I, it differed in that it mostly lacked the cells with mediolaterally oriented, dorsoventrally flattened dendritic fields that are common in lamina I. Most strikingly, it lacked the pronounced medial asymmetry of excitatory input zones and dendritic fields that characterized the lamina I population. A further distinction was that the peak synaptic response amplitudes as well as the frequency of sEPSCs were lower than in lamina I. These properties, in combination, argue for regarding the lamina I–II border cells as a distinct population within the superficial dorsal horn.

We note that the heterogeneity of the neurons in this region meant that it required a fairly substantial sample to make such a judgement. We had a high density of sampling in this region, particularly in the transverse slices, as a consequence of trying to target lamina I neurons with blind rather than visually guided patch recording. We suspect that this region was not sampled extensively in most previous slice studies, first because it represents a relatively small proportion of the superficial dorsal horn and so would not be well represented with random sampling of the superficial laminae, but also because it would be intentionally avoided in studies specifically directed at either lamina I or lamina II in order to avoid ambiguity in laminar assignment. We note that the demarcation of this as a distinct population, which does not appear to have been done previously, was based in part on differences in the patterns of local connectivity. It should be emphasized that the population is not homogeneous, and we have not identified its individual member cell types. The present line of investigation is in part a search for cell type specificity in the local circuitry of the dorsal horn, but this search is limited by the fact that only a few of the dorsal horn cell types have as yet been identified (Todd, 2010). The present results suggest that the study of circuitry can itself give clues to the identification of previously unrecognized cell types or subpopulations.

In spite of being a small and restricted population, the properties of the lamina I–II border cells suggest that they may play a critical role in interlaminar communication between superficial and deep dorsal horn. This region received both excitatory and inhibitory input from laminae III–IV, suggesting a possible role in the modulation of nociceptive processing in the superficial laminae by inputs from low-threshold mechanoreceptive A-beta fibres that project to laminae III–IV. Superficial dorsal horn neurons normally receive a low level of excitatory polysynaptic A-beta input, and the increase in this input that can occur following inflammation, nerve injury or pharmacological disinhibition may be a mechanism for mechanical pain hypersensitivity (Baba *et al.* 1999; Nakatsuka *et al.* 1999; Okamoto *et al.* 2001; Kohno *et al.* 2003; Torsney & MacDermott, 2006). Conversely, inhibitory A-beta inputs to superficial laminae could contribute to the inhibitory modulation of nociceptive transmission by tactile stimulation (Melzack & Wall, 1965).

The finding of Torsney & MacDermott (2006) that inhibitory transmitter antagonists increase the A-beta input to I–II neurons was evidence for a population of inhibitory interneurons that normally serves to reduce this A-beta input. These investigators proposed that this could occur via inhibitory interneurons that themselves receive monosynaptic A-beta input and in turn project to superficial dorsal horn neurons that receive excitatory polysynaptic A-beta input. These inhibitory interneurons were postulated to be in the vicinity of the laminae II–III border, and to project their axons into lamina II. The present results appear to be the first description of an inhibitory input from laminae III–IV to the superficial dorsal horn. Because laminae III–IV receives direct input from A-beta mechanoreceptors (Brown *et al.* 1980, 1981), this inhibitory input could potentially represent a circuit for A-beta inhibition of superficial dorsal horn neurons, and so could be one of the sources of inhibition that normally reduces excitatory A-beta input to the superficial dorsal horn. Because this deep inhibitory input was found in the subset of neurons with long ventral dendrites, and the degree of inhibitory input was correlated with the dorsoventral dendritic distribution, we postulate that it may be subserved in part via axonal connections to ventral dendrites within laminae III–IV (Fig. 7).

More generally, the present results expand on the idea that interlaminar communication from deep to superficial laminae is mediated in part by ventrally extending dendrites of superficial laminae neurons (Kato *et al.* 2009). This may be of particular importance as axonal projections from deep to superficial laminae do not appear to be a prominent feature of dorsal horn anatomy. The prior LSPS study of Kato *et al.* (2009) made maps of the photostimulation sites that produced direct (non-synaptic) responses to glutamate uncaging and used these as an indirect measure of the dendritic distribution of the postsynaptic neuron. A correlation was found between this distribution and the distribution of the excitatory synaptic input zone, in the dorsoventral but not the rostrocaudal axis, for lamina II neurons. The present study carried this further by making measurements of the dendritic fields themselves for correlations with the input zone distributions. The analysis of dendritic/synaptic correlations in the present data strengthens and extends the finding in Kato *et al.* (2009) that the distribution of excitatory inputs is correlated with the dendritic distribution, in the dorsoventral axis but not the rostrocaudal axis. The present results further showed that this correlation is also present for inhibitory inputs as well, but only for lamina I and I–II border neurons, and not the other lamina II neurons.

One way that such a correlation could come about would be if interneurons tended to seek out postsynaptic targets that are at a similar dorsoventral level to their own soma. From this preferred pool of potential targets, the selection of the actual target would then be dependent on additional factors, including the cell type of the postsynaptic neuron and whether the inputs were excitatory or inhibitory (cf. 'potential synapse' concept of Stepanyants *et al.* 2002, 2004; Shepherd *et al.* 2005; discussed in Kato *et al.* 2007). According to this idea, lamina II neurons, other than the I–II border neurons, would receive their inhibitory input from interneurons that tend to target perisomatic sites (as they have fairly uniform inhibitory

input zones that tend to be at the same dorsoventral level as their soma, and show no correlation with their dendritic distribution), whereas the I–II border neurons as well as lamina I neurons would receive inhibitory input from interneurons that tend to target dendritic sites.

An unexpected finding was the striking medial asymmetry in the excitatory synaptic input zones of lamina I neurons, which was correlated with an equally unexpected medial asymmetry in the neurons' dendrites. This asymmetry cannot be attributed to border constraints imposed by the position of the neuron's soma because the entire neuronal sample was taken from an intermediate position along the mediolateral axis of the dorsal horn. Many of the dendritic processes are truncated in the slice preparation, but we are unable to formulate a scenario that would explain how this truncation could produce such an asymmetry. Furthermore, the dendritic asymmetry is not only from lateral dendrites that terminated abruptly, but also from laterally directed dendrites that curved ventrally or medially, and so is independent of truncation. The medial asymmetry in the excitatory synaptic input zones was not solely related to dendritic asymmetry, as it was present, to a lesser degree, even for those neurons whose dendritic field was relatively symmetric. The mediolateral axis of the spinal dorsal horn represents different positions on the body; in the lumbar enlargement, medial and lateral dorsal horn represent distal and proximal hindlimb, respectively (Swett & Woolf, 1985; Bon *et al.* 2002; Takahashi *et al.* 2003). In general, there is greater sensory discrimination and an overall higher level of sensory representation of distal *versus* proximal body regions, including a higher peripheral innervation density (Mountcastle, 1957; Weinstein, 1968; Wang *et al.* 1997). The medial asymmetry we observed would result in a bias toward receiving excitatory input from more distal sites on the hindlimb, and so might be a central mechanism contributing to this enhancement of distal sensory function.

Lamina I contains a subpopulation of neurons that expresses the NK1 receptor (the receptor for the neuropeptide transmitter SP), and that plays a critical role in nociception and the development of pain hypersensitivity (Salter & Henry, 1991; Mantyh *et al.* 1997; Nichols *et al.* 1999). The NK1-positive population includes the great majority of projection neurons in lamina I, although it is not restricted to projection neurons (Littlewood *et al.* 1995; Todd *et al.* 2000; Spike *et al.* 2003; Al-Khater *et al.* 2008). We tested a sample of neurons for responsiveness to SP, as a way to identify the NK1-positive population, in order to investigate whether this population might show any differences in its local synaptic input zones. The SP-responsive neurons had excitatory input zones with a larger rostrocaudal extent than the SP-unresponsive neurons, indicating that they are capable of integrating local inputs from a relatively large area. We also found that a subset of neurons with very high sEPSC frequencies was present in the SP-responsive population. It is possible this subset includes projection neurons, as projection neurons have been found to have much higher miniature EPSC frequencies than other lamina I neurons in

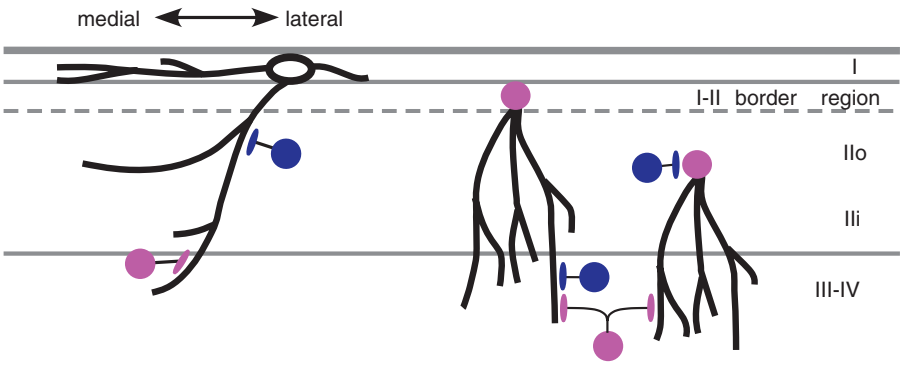

Figure 7.
Superficial dorsal horn neurons with long ventral dendrites are critical for interlaminar connectivity (schematic diagram, transverse). Neurons with long ventral dendrites have a particularly high representation among the lamina I–II border cell population, but are also present in the remainder of lamina II, as well as lamina I (although the lamina I neurons with long ventral dendrites tend to have a larger mediolateral dendritic expanse). Neurons in all three populations receive excitatory input from laminae III–IV, but only the neurons in the I–II border cell population receive substantial inhibitory input from laminae III–IV. The lamina I neurons tend to have a medial asymmetry in their dendritic fields and a corresponding asymmetry in their excitatory synaptic input zones. Thicker black lines are used to represent dendrites and axon terminals, thinner black lines represent axons. Cell bodies of inhibitory and excitatory neurons are blue and pink, respectively. Lamina II neurons with long ventral dendrites are excitatory (Yasaka *et al.* 2010), but such an analysis has not yet been done for lamina I neurons, so the lamina I cell body is uncoloured in this diagram.

the rat (Dahlhaus *et al.* 2005), although an opposite result was found when comparing sEPSC frequency in lamina I projection and non-projection neurons in the guinea pig (Grudt & Perl, 2002).

Our prior study in the rat (Kato *et al.* 2009), although it had a limited transverse sample, found that excitatory synaptic input zones of lamina II neurons were generally much wider rostrocaudally than mediolaterally, and this was also found in the present study. The previous study also found that the excitatory input zones of lamina II neurons were much wider rostrocaudally than their inhibitory input zones, which suggested that local circuitry might not be sufficient to account for the large inhibitory receptive fields often found for dorsal horn neurons (discussed in Kato *et al.* 2011). Our present results showed an opposite but much smaller difference in the mediolateral axis, where the inhibitory input zones are slightly (30%) wider than the excitatory input zones, in lamina II neurons (excluding the lamina I–II border cells). This difference might contribute to some degree of surround inhibition, but nonetheless the inhibitory input zones are fairly restricted, and so it would still appear that descending inhibition would be required to account for the very widespread inhibitory influences commonly found in dorsal horn neurons (Hillman & Wall, 1969; Kato *et al.* 2011).

References

Al-Khater KM, Kerr R & Todd AJ (2008). A quantitative study of spinothalamic neurons in laminae I, III, and IV in lumbar and cervical segments of the rat spinal cord. *J Comp Neurol* **511**, 1–18.

Baba H, Doubell TP & Woolf CJ (1999). Peripheral inflammation facilitates A-beta fiber-mediated synaptic input to the substantia gelatinosa of the adult rat spinal cord. *J Neurosci* **19**, 859–867.

Boada MD & Woodbury CJ (2008). Myelinated skin sensory neurons project extensively throughout adult mouse substantia gelatinosa. *J Neurosci* **28**, 2006–2014.

Bon K, Wilson SG, Mogil JS & Roberts WJ (2002). Genetic evidence for the correlation of deep dorsal horn Fos protein immunoreactivity with tonic formalin pain behavior. *J Pain* **3**, 181–189.

Braz JM, Nassar MA, Wood JN & Basbaum AI (2005). Parallel "pain" pathways arise from subpopulations of primary afferent nociceptor. *Neuron* **47**, 787–793.

Brown AG, Fyffe RE & Noble R (1980). Projections from Pacinian corpuscles and rapidly adapting mechanoreceptors of glabrous skin to the cat's spinal cord. *J Physiol* **307**, 385–400.

Brown AG, Fyffe RE, Rose PK & Snow PJ (1981). Spinal cord collaterals from axons of type II slowly adapting units in the cat. *J Physiol* **316**, 469–480.

Callaway EM & Katz LC (1993). Photostimulation using caged glutamate reveals functional circuitry in living brain slices. *Proc Natl Acad Sci U S A* **90**, 7661–7665.

Craig AD & Kniffki KD (1985). Spinothalamic lumbosacral lamina I cells responsive to skin and muscle stimulation in the cat. *J Physiol* **365**, 197–221.

Dahlhaus A, Ruscheweyh R & Sandkühler J (2005). Synaptic input of rat spinal lamina I projection and unidentified neurones in vitro. *J Physiol* **566**, 355–368.

Galhardo V & Lima D (1999). Structural characterization of marginal (lamina I) spinal cord neurons in the cat: a Golgi study. *J Comp Neurol* **414**, 315–333.

Grudt TJ & Perl ER (2002). Correlations between neuronal morphology and electrophysiological features in the rodent superficial dorsal horn. *J Physiol* **540**, 189–207.

Hillman P & Wall PD (1969). Inhibitory and excitatory factors influencing the receptive fields of lamina 5 spinal cord cells. *Exp Brain Res* **9**, 284–306.

Kato G, Kawasaki Y, Ji RR & Strassman AM (2007). Differential wiring of local excitatory and inhibitory synaptic inputs to islet cells in rat spinal lamina II demonstrated by laser scanning photostimulation. *J Physiol* **580**, 815–833.

Kato G, Kawasaki Y, Koga K, Uta D, Kosugi M, Yasaka T, Yoshimura M, Ji RR & Strassman AM (2009). Organization of intralaminar and translaminar neuronal connectivity in the superficial spinal dorsal horn. *J Neurosci* **29**, 5088–5099.

Kato G, Kosugi M, Mizuno M & Strassman AM (2011). Separate inhibitory and excitatory components underlying receptive field organization in superficial medullary dorsal horn neurons. *J Neurosci* **31**, 17300–17305.

Katz LC & Dalva MB (1994). Scanning laser photostimulation: a new approach for analyzing brain circuits. *J Neurosci Meth* **54**, 205–218.

Kohno T, Moore KA, Baba H & Woolf CJ (2003). Peripheral nerve injury alters excitatory synaptic transmission in lamina II of the rat dorsal horn. *J Physiol* **548.1**, 131–138.

Light AR & Perl ER (1979). Spinal termination of functionally identified primary afferent neurons with slowly conducting myelinated fibers. *J Comp Neurol* **186**, 133–150.

Light AR, Sedivec MJ, Casale EJ & Jones SL (1993). Physiological and morphological characteristics of spinal neurons projecting to the parabrachial region of the cat. *Somatosens Mot Res* **10**, 309–325.

Lima D & Coimbra A (1986) A Golgi study of the neuronal population of the marginal zone (lamina I) of the rat spinal cord. *J Comp Neurol* **244**, 53–71.

Littlewood NK, Todd AJ, Spike RC, Watt C & Shehab SA (1995). The types of neuron in spinal dorsal horn which possess neurokinin-1 receptors. *Neuroscience* **66**, 597–608.

Lu Y & Perl ER (2003). A specific inhibitory pathway between substantia gelatinosa neurons receiving direct C-fiber input. *J Neurosci* **23**, 8752–8758.

Lu Y & Perl ER (2005). Modular organization of excitatory circuits between neurons of the spinal superficial dorsal horn (laminae I and II). *J Neurosci* **25**, 3900–3907.

Luz LL, Szucs P, Pinho R & Safronov BV (2010). Monosynaptic excitatory inputs to spinal lamina I anterolateral-tract-projecting neurons from neighbouring lamina I neurons. *J Physiol* **588**, 4489–4505.

Mantyh PW, Rogers SD, Honore P, Allen BJ, Ghilardi JR, Li J, Daughters RS, Lappi DA, Wiley RG & Simone DA (1997). Inhibition of hyperalgesia by ablation of lamina I spinal neurons expressing the substance P receptor. *Science* **278**, 275–279.

Melzack R & Wall PD (1965). Pain mechanisms: a new theory. *Science* **150**, 971–979.

Mountcastle VB (1957). Modality and topographic properties of single neurons of cat's somatic sensory cortex. *J Neurophysiol* **20**, 408–434.

Nakatsuka T, Park J-S, Kumamoto E, Tamaki T & Yoshimura M (1999). Plastic changes in sensory inputs to rat substantia gelatinosa neurons following peripheral inflammation. *Pain* **82**, 39–47.

Nichols ML, Allen BJ, Rogers SD, Ghilardi JR, Honore P, Luger NM, Finke MP, Li J, Lappi DA, Simone DA & Mantyh PW (1999). Transmission of chronic nociception by spinal neurons expressing the substance P receptor. *Science* **286**, 1558–1561.

Okamoto M, Baba H, Goldstein PA, Higashi H, Shimoji K & Yoshimura M (2001). Functional reorganization of sensory pathways in the rat spinal dorsal horn following peripheral nerve injury. *J Physiol* **532.1**, 241–250.

Salter MW & Henry JL (1991). Responses of functionally identified neurones in the dorsal horn of the cat spinal cord to substance P, neurokinin A and physalaemin. *Neuroscience* **43**, 601–610.

Schneider SP (2008). Local circuit connections between hamster laminae III and IV dorsal horn neurons. *J Neurophysiol* **99**, 1306–1318.

Shepherd GMG, Stepanyants A, Bureau I, Chklovskii D & Svoboda K (2005). Geometric and functional organization of cortical circuits. *Nat Neurosci* **8**, 782–790.

Spike RC, Puskár Z, Andrew D & Todd AJ (2003). A quantitative and morphological study of projection neurons in lamina I of the rat lumbar spinal cord. *Eur J Neurosci* **18**, 2433–2448.

Stepanyants A, Hof PR & Chklovskii DB (2002). Geometry and structural plasticity of synaptic connectivity. *Neuron* **34**, 275–288.

Stepanyants A, Tamas G & Chklovskii DB (2004). Class-specific features of neuronal wiring. *Neuron* **43**, 251–259.

Sugiura Y, Lee CL & Perl ER (1986). Central projections of identified, unmyelinated (C) afferent fibers innervating mammalian skin. *Science* **234**, 358–361.

Swett JE & Woolf CJ (1985). The somatotopic organization of primary afferent terminals in the superficial laminae of the dorsal horn of the rat spinal cord. *J Comp Neurol* **231**, 66–77.

Takahashi Y, Chiba T, Kurokawa M & Aoki Y (2003). Dermatomes and the central organization of dermatomes and body surface regions in the spinal cord dorsal horn in rats. *J Comp Neurol* **462**, 29–41.

Todd AJ (2010). Neuronal circuitry for pain processing in the dorsal horn. *Nat Rev Neurosci* **11**, 823–836.

Todd AJ, McGill MM & Shehab SA (2000). Neurokinin 1 receptor expression by neurons in laminae I, III and IV of the rat spinal dorsal horn that project to the brainstem. *Eur J Neurosci* **12**, 689–700.

Torsney C & MacDermott AB (2006). Disinhibition opens the gate to pathological pain signaling in superficial neurokinin 1 receptor-expressing neurons in rat spinal cord. *J Neurosci* **26**, 1833–1843.

Wang L, Millecchia R & Brown PB (1997). Correlation of peripheral innervation density and dorsal horn map scale. *J Neurophysiol* **78**, 689–702.

Weinstein S (1968). Intensive and extensive aspects of tactile sensitivity as a function of body part, sex, and laterality. In *The Skin Senses*, ed Kenshalo DR, pp 195–222. Thomas, Springfield, IL.

Willis WD & Coggeshall RE (2004). *Sensory Mechanisms of the Spinal Cord*, 3rd edn. Kluwer Academic, New York.

Woodbury CJ & Koerber HR (2003). Widespread projections from myelinated nociceptors throughout the substantia gelatinosa provide novel insights into neonatal hypersensitivity. *J Neurosci* **23**, 601–610.

Yasaka T, Kato G, Furue H, Rashid MH, Sonohata M, Tamae A, Murata Y, Masuko S & Yoshimura M (2007). Cell-type-specific excitatory and inhibitory circuits involving primary afferents in the substantia gelatinosa of the rat spinal dorsal horn in vitro. *J Physiol* **581**, 603–618.

Yasaka T, Tiong SY, Hughes DI, Riddel JS, Todd AJ (2010). Populations of inhibitory and excitatory interneurons in lamina II of the adult rat spinal dorsal horn revealed by a combined electrophysiological and anatomical approach. *Pain* **151**, 475–488.

Zhang W & Schneider SP (2011). Short-term modulation at synapses between neurons in laminae II-V of the rodent spinal dorsal horn. *J Neurophysiol* **105**, 2920–2930.

Zheng J, Lu Y & Perl ER (2010). Inhibitory neurones of the spinal substantia gelatinosa mediate interaction of signals from primary afferents. *J Physiol* **588**, 2065–2075.

Zylka MJ, Rice FL & Anderson DJ (2005). Topographically distinct epidermal nociceptive circuits revealed by axonal tracers targeted to Mrgprd. *J Neurosci* **45**, 17–25.

Author contributions

The experiments were performed in the laboratory of A.M.S. M.K., G.K. and A.M.S. designed the experiments and drafted the paper. M.K., G.K., S.L., M.K. and A.M.S. contributed to collection, analysis and interpretation of the data. All authors approved the final version of the manuscript.

Acknowledgement

This work was supported by NIH grant R01 NS057454 to A.M.S. The authors declare no competing financial interest.